Journal Pre-proof

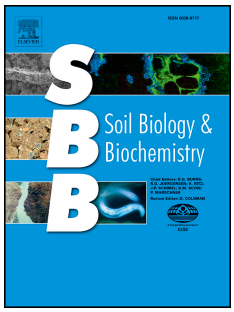

Thermodynamics of Microbial Decomposition of Persistent Carbon in Erosion-Buried Topsoils

Mitchell A.D., Helgason B.L

PII: S0038-0717(25)00002-1

DOI: https://doi.org/10.1016/j.soilbio.2025.109710

Reference: SBB 109710

To appear in: *Soil Biology and Biochemistry*

Received Date: 8 August 2024

Revised Date: 20 December 2024

Accepted Date: 4 January 2025

Please cite this article as: Mitchell, A.D, B.L, H., Thermodynamics of Microbial Decomposition of Persistent Carbon in Erosion-Buried Topsoils, *Soil Biology and Biochemistry*, https://doi.org/10.1016/j.soilbio.2025.109710.

Thermodynamics of Microbial Decomposition of Persistent Carbon in Erosion-Buried Topsoils

Mitchell, A.D.[1*], Helgason, B.L[1]

[1] Department of Soil Science, College of Agriculture and Bioresources, University of Saskatchewan, 51 Campus Dr., Saskatoon, SK, Canada S7N 5A8

[*]Corresponding Author: B.L. Helgason, 51 Campus Dr., Saskatoon, SK, S7N 5A8 Tel: +1 306 966 8151 e-mail address: bobbi.helgason@usask.ca

Keywords: Buried C, SOC Persistence, Thermodynamic Efficiency, Microbial Community Composition, C Cycling

Abstract

Hillslope erosion in hummocky landscapes can lead to the accumulation of C-rich topsoil in depositional positions that eventually becomes buried if erosion persists. Our objective in this study was to evaluate the persistence of SOC and the thermodynamic efficiency of the microbial community in C-rich buried surface horizons from five sites with varied texture and organic matter contents. Surface Ah (0-10 cm) and buried surface (Ahb) horizons were isolated from intact cores, sieved (<2 mm) and incubated under ideal conditions of temperature and moisture. Ahb soils had an average organic C content (25.6 mg OC g^{-1} soil) similar to the corresponding Ah soil (30.9 mg OC g^{-1} soil). Using isothermal calorimetry, we determined that Ah horizons produced significantly more heat and CO_2 but had smaller calorespirometric ratios than Ahb soils, under both basal (841 vs 3106 kJ mol^{-1} CO_2-C) and glucose metabolism (627 vs. 697 kJ mol^{-1} CO_2-C).100-day basal respiration was nearly four times greater in Ah vs. Ahb horizons. While MAOM correlated with basal heat production in both horizons, it only correlated with C persistence in the Ah horizons (Rho = 0.67, $p < 0.01$), suggesting variability in C persistence was not primarily driven by organo-mineral bonds in Ahb horizons, although energy use efficiency is. Microbial community structure in Ahb horizons was distinct from the surface soils, and changed minimally during incubation, suggesting co-development of the community as decomposition proceeded over the decades of burial, leading to persistent C. These relatively large volume buried surface soils may provide unique opportunities to understand microbial hotspot C processes that are typically difficult to isolate at a spatially explicit scale (e.g., an aggregate interior). We propose that the co-development of distinct microbial communities in C-rich buried horizons leads to more thermally stable SOC, but further research is required to test this hypothesis.

1. Introduction

The re-distribution of soil due to erosion can lead to burial of the original soil profile in depositional areas (Van Oost et al., 2005). The more recently deposited material creates an inverted soil profile when deposition of eroded topsoil and eventually, sub-soil, from upper slope positions is deposited in the lower concave position (Berhe et al., 2008). Additionally, surface soils may be buried through volcanic, alluvial and aeolian burial processes (Chaopricha and Marín-Spiotta, 2014). Buried surface horizons have been found to store concentrations of C similar to corresponding at-surface horizons in depositional positions following decades of landscape stabilization (Chaopricha and Marín-Spiotta, 2014; VandenBygaart et al., 2012). This former surface C was more stable and had longer mean residence times than other subsoils in non-eroding soil profiles (Doetterl et al., 2012; Z. Wang et al., 2014; Alcántara et al., 2017) and/or corresponding new surface horizons (Wang et al., 2013; VandenBygaart et al., 2015). Erosion- buried surface soils were developed under very similar soil forming factors as they developed at the same site having the same parent material, climate, and topography as their corresponding surface horizons. Comparison of erosion-buried surface horizons to corresponding surface horizons provides a unique opportunity to study the effects on soil organic carbon (SOC) and microbial communities when the soil is buried for decades and fresh C inputs are reduced.

The persistence of SOC in soils is often reliant on protection from microbial mineralization through occlusion of organic matter within aggregates (Su et al., 2023), through organo-mineral bonds (Salomé et al., 2010; Schrumpf et al., 2013), and due to the composition of the SOC (Lehmann et al., 2020). Disruption to aggregates by soil sieving prior to incubation was shown to increase C mineralization in subsoils more than topsoils (Salomé et al., 2010), however crushing of aggregates in buried surface horizons had little effect on C mineralization (X. Wang et al.,

2014), suggesting that aggregation has little effect on the C stability observed in the buried topsoils. Organo-mineral bonds are dependent on reactive soil surfaces, therefore soils with a greater proportion of clay tend to store more mineral-associated organic matter (MAOM) (Kögel-Knabner et al., 2008). Buried topsoils have been shown to store a greater proportion of C as MAOM than surface horizons at depositional sites, however texture can play an important role in MAOM formation and soil textures were not examined in these studies (X. Wang et al., 2014; Doetterl et al., 2015). Concomitantly, buried topsoils have also been shown to store more light fraction C than surface horizons, despite containing more persistent C (VandenBygaart et al., 2015). Substantial viable microbial biomass has been found in buried surface horizons (Helgason et al., 2014), suggesting that there is accessible C and energy, despite the fact that new C inputs are mainly limited to vertically transported soluble C and/or direct root C deposition. Traditional theories regarding C protection being driven by aggregation, mineral-association, and reduced microbial activity do not appear to sufficiently explain the C persistence observed in these buried surface horizons, however functional complexity of SOC in buried surface horizons has not been examined.

More recent literature on C cycling discusses organic matter not only as a source of C, but also a source of energy (Gunina and Kuzyakov, 2022). Gunina and Kuzyakov (2022) proposed that with each breakdown, SOM becomes increasingly concentrated in energy, although that energy becomes more challenging to access. Examining the energy use efficiency (EUE) of the microbial community, which is defined by the proportion of energy from a C substrate used for growth and maintenance processes (Wang and Kuzyakov, 2023), can elucidate links between microbial metabolism and energy stored in SOM (Barros et al., 2016).

Past research has shown repeated microbial turnover of C in buried surface horizons (Hobara et al., 2020) leading to C resistant to mineralization to CO_2 (VandenBygaart et al., 2015; Doettrel et al., 2012; Wang et al. 2013). Repeated microbial turnover also occurs in microbial "hotspots" which are areas in soil where organic C and microorganisms interact, such as within microsites like the rhizosphere, on the surface of and within aggregates, or on the surface of plant residues (Kuzyakov and Blagodatskaya, 2015). While many studies are using ^{13}C tracing to identify and examine microbial hotspots or isolate rhizosphere soil (Huang et al., 2020; Lange et al., 2024), it remains challenging to isolate persistent C from these areas. Buried surface horizons may present a unique opportunity to study soils in this state of advanced decomposition" because similar to hotspots, they were buried with high concentrations of C, have experienced minimal physical disturbance, and receive limited fresh C inputs but have been shown to contain very persistent C which has undergone repeated microbial turnover.

To our knowledge, ours is the first study to examine the thermodynamics of microbial communities in buried surface horizons explicitly. Here we characterize microbial community composition, mineralizable C and soil energetics in buried surface horizons during incubation under controlled conditions. The buried surface horizons and corresponding current surface horizons originated from arable soils at five different sites with varying soil textures and climate conditions that have affected the quantity and composition of SOM. Our objective was to investigate the dynamics of SOC cycling under controlled conditions in buried surface horizons, relative to the corresponding newly formed surface horizons, to better understand persistent C formation and to link microbial C cycling and energetics under basal and glucose amended conditions. We hypothesized that 1) SOC in buried surface horizons (referred to as Ahb horizons) would be more resistant to mineralization to CO_2 in soils regardless of the soil texture,

indicating that mineral association is not the only mechanism driving C persistence in these soils; 2) larger calorespirometric ratios from both indigenous SOC and added glucose experiments in Ahb horizons are driven by an increased proportion of persistent SOC coupled with an adapted microbial community that co-developed following decades of burial; and 3) heat dissipation is positively correlated with increased proportion of organo-minerals bonds which requires increased energy input to access (Gregorich et al, 2015), decreasing the energy use efficiency of the microbial community.

2. Methods

2.1. *Soil sampling and handling for analysis*

Samples were collected in the fall of 2021 following harvest on Oct. 18 at St. Denis National Wildlife Area (SDNWA), Oct. 22 at Bruno and Cudworth, Nov. 5 at Gronlid, and in the spring of 2022 before seeding on Apr. 23 at Swift Current. There was no snow cover when sites were sampled, and ground temperature was below 10°C. Sites were developed under varying vegetation native to each ecoregion as reported in Table 1 and, except for St. Denis, are all currently managed under annual cropland. Sites are believed to have been converted to annual cropland around the same time in the early 1900s, including St. Denis, which was only converted back to grassland between 2013 and 2016. Four replicate samples were collected 2 m apart at each site, near the base of the hillslope. For each replicate sample, three adjacent soil cores were taken parallel with the hillslope about 6 cm apart and pooled. Ah horizon soil was collected from the 0- to 10-cm depth. The buried surface horizon, henceforth referred to as the Ahb horizon, was collected based on the color change observed as darker colored soil in buried surface horizons. A fourth core was collected at each sample position (n=4) for bulk density determination. Field-moist soil samples were stored under refrigeration overnight and processed

within 24 h of collection by passing through a 2-mm sieve. Sub-samples taken for phospholipid fatty acid analysis (PLFA) were immediately frozen at -20°C. Samples for PLFA analysis were freeze-dried using the liquid N snap freeze method by an Alpha 1-2 LD freeze drier. All remaining soil was stored at 4°C for C mineralization and isothermal calorimetry experiments and a small sub-sample was air-dried for SOC analysis

2.2. *Field soil characteristics*

Soil organic C analysis was performed by dry combustion at 1350 °C on a LECO C632 analyzer (*LECO Corporation, St. Joseph, MI, USA*). Samples were air-dried and ground to <250 μm using a mechanical ball grinder before being pre-treated with H_2SO_3 prior to analysis to remove inorganic C according to the method outlined by Skjemstad and Baldock (2008). Sand, silt, clay contents were determined using the hydrometer method (Kroetsch and Wang, 2008). Soil pH was measured using a pH meter at a soil-to-water ratio of 1:1 (w/v) (Hendershot et al., 2008).

Gravimetric water content (GWC) was determined by measuring mass lost on a 10 g sub-sample of soil dried at 105°C for 24-h. Bulk density was determined by recording the weight of total field moist soil collected from each bulk density core. The sample was air-dried and passed through a 2 mm sieve. The weight of all rocks that would not pass through a 2 mm sieve was recorded and subtracted from the total weight of the field moist sample. The dry soil weight was then calculated based on GWC and used for bulk density calculation by dividing by the volume of the core. The height of each core was recorded in field as the depth increment sampled, ie. 10 cm for Ah horizons where the 0- to 10- cm depth was collected, while Ahb horizons were variable between site and replicate based on the darker colour observed.

Phospholipid fatty acid (PLFA) extraction was performed using to the modified high-throughput method described by Ellis and Ritz (2018). Briefly, fatty acids were extracted from 2.5 g of freeze-dried, mortar and pestle ground soil using Bligh-Dyer extractant solution and separated using a solid phase extraction column (50 mg Si, HyperSep^{TM,} ThermoScientifc, USA). Fatty acids were then methylated, and a known quantity of internal standard (methyl nonadecanoate; 19:0) was added to each sample for quantification purposes. Fatty acid methyl-esters (FAMEs) were identified based on a library of known FAME retention indices on a Bruker 436 GC equipped with a flame ionization detector (FID) (Bruker Corporation, Billerica, MA). Known PLFA biomarkers were used to identify microbial groups: Fungi were identified as 18:2ω6,9, AMF were identified by 16:1ω5c, total bacteria were calculated as the sum of Gram positive (GP) bacteria (i14:0, i15:0, a15:0, i16:0, i17:0, a17:0), Gram negative (GN) bacteria (16:1ω7t, 16:1ω9c, 16:1ω7c, 18:1ω7c, 18:1ω9c, cy17:0, and cy19:0) and actinobacteria (16:0 10-methyl and 18:0 10-methyl). The stress-1 biomarker was calculated as the ratio of cy17:0 to 16:1ω7c and stress-2 was calculated as the ratio of cy19:0 to 18:1ω7c (Helgason et al., 2010; Wixon and Balser, 2013). The ratio of fungi to bacteria was calculated by comparing total 18:2ω6,9 to the sum of Gram positive, Gram negative and Actinobacteria biomarkers.

Amino sugar extraction and quantification was preformed according to Indorf et al. (2011). Briefly, 400 mg to 500 mg freeze-dried, mortar and pestle ground soil was mixed with 5 mL of 6 M HCl in anaerobic conditions created by flushing a hand-in-bag artificial atmospheric chamber (Spilfyter ®, NPS Corp) four times with N before capping vials. After 6-hours of hydrolysis at 105°C the samples were filtered over glass microfiber filters (Whatman GF/F) and filtrates were transferred via glass pipette into 4 mL GC vials to be stored at 4°C until purification. A 0.3 mL aliquot was evaporated to dryness at 40-45°C under a continuous N flow at 2 psi to remove HCl.

Samples were re-dissolved in 0.5 mL MilliQ water and evaporated a second time under the same conditions before finally being re-dissolved in 1 mL MilliQ water. Samples were vortexed briefly and transferred to a 2 mL GC vial and stored at 4°C until detection on an Agilent 1260 Infinity II HPLC (Agilent Technologies, Santa Clara, CA, USA) equipped with an Agilent 1260 Infinity II fluorescent detector (Model G7121A) set at 455 nm emission and 350 nm excitation wavelength. An Infinity II Vialsampler (Model G7129A) was added for autosampling due to the need for precision during derivatization, where a 50 uL sample of derivatization reagent, prepared according to Indorf et al. (2011), and 30 μL of sample were mixed inside the injection loop and following 120s of reaction time, 15 μL of indole derivatives were injected for separation on a Phenomenex (Aschaffenburg, Germany) Hyperclone C_{18} (ODS) column (125 mm in length x 4 mm diameter x 5 μm particle size) protected by a Phenomenex C_{18} security guard cartridge (4 mm length x 2 mm diameter). The mobile phase consisted of two eluents, A and B (Indorf et al., 2011), which were run isocratically in a 93/7 (v/v) ratio of eluent A/B at a flow rate of 1.5 mL min^{-1} during amino sugar separation for 19 min. Glucosamine (GluN), Galactosamine (GalN) and Muramic Acid (MurA) were quantified based on the peak area and retention times of an added known quantity of external samples of glucosamine and muramic acid.

We estimated fungal and bacterial necromass C based on equations described by Appuhn and Joergensen (2006) and Joergensen (2018) where bacterial necromass C was equal to concentrations of MurA multiplied by a factor of 45, and fungal necromass C:

$$Fungal\ necromass\ C\ = \left(\left(\frac{GluN}{179.12} - 2\ X\ \left(\frac{MurA}{251.23} \right) \right) x\ 179.17\ x\ 9 \right) \quad (1)$$

Where 179.12 g mol^{-1} and 251.23 g mol^{-1} are the molecular weights of GluN and MurA, respectively, an assumed molar ratio of 1:2 of MurA to GluN in bacterial cells (Engelking et al., 2007), and 9 is the conversion value of fungal GluN to fungal necromass C (Appuhn and Joergensen, 2006; Joergensen, 2018).

The proportion of mineral-associated organic matter C was determined using a particle size separation method from Cambardella and Elliot (1992) and Haddix et al. (2020). Briefly, ten grams of air-dried soil was shaken with 35 mL of deionized H_2O for 15 minutes then centrifuged at 1069 g for 30 minutes. The resulting supernatant was removed, and 2 g of glass beads and 35 mL of 0.5% Sodium hexametaphosphate $(NaPO_3)_6$ solution was added to each tube before being shaken for 18-h on an end over end shaker. Following shaking, samples were poured onto a 53μm sieve and rinsed with deionized H_2O to help the MAOM pass through the sieve. The MAOM that passed through the sieve was transferred to an aluminum tray lined with parchment paper and placed in the oven to dry at 70°C. Sampled were ground using a ball grinder, then analyzed for SOC content by pre-treating with H_2SO_3 and dry combusting at 1350°C using a LECO C632 analyzer (*LECO Corporation, St. Joseph, MI, USA*). We had a C recovery efficiency of 72% - 97%, slightly lower than other ranges reported in literature (Haddix et al., 2020).

2.3. Soil microbial Carbon mineralization experiments

A closed-vessel incubation was conducted to determine the potentially mineralizable C present in Ah and Ahb horizons (VandenBygaart et al., 2015). Briefly, soil microcosms were constructed using 50 g dw soil adjusted to 60% WHC placed into 30-dram vials (4.6 cm Ø). Vials were then pre-incubated at 25°C for 7-days prior to the beginning of the experiment. At the beginning of the experiment, vials were placed in separate air-tight 1 L glass mason jars fitted

with a rubber septum for gas sampling. The headspace of all jars was flushed with CO_2 free compressed air (1 L min^{-1}) for 7 minutes at the initiation of the experiment and immediately after each headspace sampling event.

The amount of CO_2 present in the headspace of each jar was determined by collecting 10 mL of air using an air-tight syringe and injecting into a Licor 7000 (Licor, Lincoln, NE, USA). Air in the headspace of each jar was mixed by filling and decompressing the air-tight syringe three to four times and then letting rest for about ten seconds before removing 10 mL of air for sampling. Measurements were repeated and the average of the two measurements was used in the calculation. Measurements were taken on days 1, 2, 3, 7, twice weekly until day 42, and then weekly until day 100. Samples were adjusted to 60% WHC by weight after each gas sampling event. Following the 100-days of incubation, microcosms were sub-sampled, freeze-dried and stored at -20°C before undergoing PLFA analysis as described in 2.2 Field Soil Characteristics.

2.4. *Isothermal calorimetry experiments*

The energetic efficiency of the microbial communities during decomposition of the indigenous SOM and added glucose was assessed using isothermal calorimetry (Herrmann et al., 2014). Briefly, 5 g of soil was packed to field bulk density and pre-incubated at 25°C for 14 days 45% WHC in 20 mL glass ampoules specifically for calorimetry. The TAM Air instrument used has eight channels, requiring that the experiments were run in batches. Each experiment contained two field replicates of Ah and Ahb soils. Two replicate ampoules for each soil were pre-incubated per experiment and amended with either glucose or water at the beginning of the experiment. The glucose-amended treatment received 500 μg C g^{-1} soil as glucose dissolved in sterilized MilliQ water, and the basal treatment received sterilized MilliQ water only, bringing the water content of each sample to 65% WHC. Ampoules were immediately sealed and placed

in an eight channel TAM Air calorimeter (TA Instruments, Sollentuna, Sweden). After a 45 min stabilization period, as required before signal can be considered correct (TA Instruments, 2012), heat flow was continuously measured for 48 h at 25°C. An ampoule filled with sterilized milli-Q water calculated to contain water equal to the equivalent heat capacity as the calculated 5 g of soil adjusted to 65% WHC for each horizon at each site was used as a reference ampoule and introduced into the machine prior to collecting a stabilized baseline before each experiment was initiated.

At end of the 48-h experiment, ampoules were removed from the calorimeter, and 20 mL of CO_2-free air was introduced into each ampoule to pressurize the headspace. The headspace of each ampoule was thoroughly mixed by plunging the syringe three times, and a 10 mL sample of air was removed to measure CO_2 concentrations on a Licor Li-7000 (Licor, Lincoln, NE, USA). An additional ampoule free of soil was sealed at the beginning of the experiment and kept at 25°C until time of headspace sampling of the soil-filled ampoules, where 20 mL of air was added to headspace and sampled to determine initial background concentrations of CO_2 in experiment ampoules.

Thermodynamic efficiency (η_{eff}) of soil microbial communities was calculated based on the equation from Harris et al. (2012) which assumes total utilization of added C substrates during the incubation period:

$$\eta_{eff} = 1 - \frac{Q_{glucose} - Q_{basal}}{\Delta H_{glucose}} \quad (2)$$

Where η_{eff} is the thermodynamic efficiency of the soil, $Q_{glucose}$ is the heat produced from glucose-amended soils (J g^{-1} soil), Q_{basal} is the heat produced from water-amended soils (J g^{-1} soil) and $\Delta H_{glucose}$ is the combustion enthalpy of the added glucose (J g^{-1} soil), which is 2816.8 kJ mol^{-1}. A total of 19.5 J g^{-1} soil of glucose was added to each glucose-amended vial.

2.5. Statistical analysis

Statistical differences between means were analyzed using the lme function from the nlme package (version 3.1.153) in R for differences between Ah and Ahb horizons. The lme function is a linear mixed effects model that allows specification of fixed and random factors to specify how samples are not independent for examining differences between means of specified groups. Horizon was set as the fixed factor, site and rep were set as random factors. Post-hoc testing was performed using a TukeyHSD post-hoc test. Residuals were examined and data was log-transformed if non-normality was observed to satisfy assumptions of the model for isothermal calorimetry, C mineralization, microbial functional groups, and SOC data. Data was analyzed using a 1-way ANOVA with a TukeyHSD post-hoc test to determine differences between means of Ah and Ahb horizons within a site. Log-transformation was performed if necessary. All PLFA data was log-transformed ($\chi + 1$) prior to analysis. Spearman correlation coefficients were used to examine relationships of C mineralization and isothermal calorimetry measures with microbial functional groups, abundance, and necromass, SOC, and soil texture.

Non-metric multi-dimensional scaling (NMDS) ordination was performed on Bray-Curtis dissimilarity indices calculated on log-transformed ($\chi + 1$) mol% PLFA data. Differences in community structure were examined using a PERMANOVA from the adonis function in the vegan 2.6.4 package (Oksanen et al., 2022) in R 4.1.2 (R Development Core Team, 2021).

3. Results

3.1. *Soil organic matter persistence between Ah and Ahb horizons*

Soil organic C was less susceptible to mineralization to CO_2 over the course of 100-days of incubation in the Ahb horizon vs. Ah horizon despite having similar SOC concentrations (Ah = 30.9 ± 2.05 mg OC g^{-1} soil; Ahb = 25.8 ± 2.90 mg OC g^{-1} soil) (Table 2). Specifically, Ah

horizons mineralized nearly four times as much CO_2 (0.96 ± 0.05 mg CO_2-C g^{-1} soil) than Ahb horizons (0.22 ± 0.02 mg CO_2-C g^{-1} soil). Thus, when the amount of CO_2 mineralized over 100-days was normalized to the OC content, Ah horizons also mineralized nearly four times the proportion of C (35.0 ± 2.76 mg CO_2-C g^{-1} OC) than the Ahb horizon (9.1 mg ± 0.63 CO_2-C g^{-1} OC) (Fig. 1a).

Despite significant differences in the abundance of the microbial community between Ah and Ahb horizons after 100-days of incubation (Fig. 2), mineralized CO_2 per unit of PLFA in the Ah horizon (0.023 mg CO_2 $nmol^{-1}$ PLFA) was twice that produced by the Ahb horizon (0.011 mg CO_2 $nmol^{-1}$ PLFA) (Fig. 1b). While there were significant differences in total microbial abundance in the field (Table 2) and after 100-days of incubation (Fig. 2), there was no difference in the concentration of fungal necromass between the Ah and Ahb horizons in the field; however, there was significantly less bacterial necromass in Ahb horizons (Table 2).

While microbial abundance after 100-days of incubation was correlated with differences in potentially mineralizable C (Rho = 0.53, $p < 0.01$), this did not fully account for differences in CO_2 production between horizons (Fig. 1b), indicating that in addition to microbial abundance, community structure may have played an important role. Non-metric multi-dimensional scaling (NMDS) analysis of PLFA profiles from soils after 100-days of incubation resulted in a 2-D solution (final stress = 0.13) which showed a clear separation of horizon on axis 1 (Fig. 2). Horizon was strongly correlated with axis 1 (Rho = 0.86, $p < 0.0000001$).

Correlation between Ah horizon communities and GN bacteria (Rho = 0.65, $p < 0.00001$), fungi (Rho = 0.75, $p < 0.00001$), and the fungal to bacterial ratio (Rho = 0.74, $p < 0.00001$) reflects the contribution of these functional groups to Ah horizon community structure. Similarly, actinomycetes (Rho = -0.87, $p < 0.00001$) correlated with the Ahb horizon

community. Further, strong positive correlations existed between mineralized CO_2 per g OC and fungi (Rho = 0.69, $p < 0.001$), F:B ratio (Rho = 0.68, $p < 0.001$), and strong negative correlations with actinobacteria (Rho = -0.72, $p < 0.001$), suggesting greater mineralization from soils with more fungi and less actinobacteria. There were also correlations between potentially mineralizable C and the relative abundance of other groups such as GN bacteria (Rho = 0.36, $p < 0.05$), and negative correlations with GP bacteria (Rho = -0.36, $p < 0.05$) and AMF (Rho = -0.41, $p < 0.05$). There were no significant correlations between soil texture and potentially mineralizable C between the Ah and Ahb horizons.

The conditions of the incubation (i.e., 60% WHC at 25°C, flushed with CO_2-free air after each sampling period ensuring aerobic conditions), may not be conditions experienced in the field. This change in environment had a greater effect on Ah horizons, decreasing total PLFA by 42% after 100-days of incubation compared to only a 19% decrease in Ahb horizons (Table 3). There was also a shift in the microbial community composition with GP bacterial abundance increasing by 27% after 100-days of incubation in the Ah horizon compared to 12% in the Ahb horizon, and fungal to bacterial ratio decreasing by 46% in the Ah horizon compared to only 18% in the Ahb horizon. The relative abundance of GN bacteria changed similarly between the Ah and Ahb horizon, changing by a range of a 9.18% decrease to a 6.95% increase across all sites.

Soil texture played a significant role in the persistence of C in the Ah horizon from Cudworth (63% sand) and Gronlid (57% sand) which mineralized a greater proportion of C (51.1 ± 2.37 mg CO_2-C g^{-1} OC; 35.9 ± 1.98 mg CO_2-C g^{-1} OC, respectively) compared to Bruno (39% sand, 35% clay) which only mineralized 19.1 ± 0.89 mg CO_2-C g^{-1} OC (Fig. 3a). Despite similar textural classifications, there was a strong correlation between the amount of CO_2 g^{-1} OC

produced with the proportion of sand in the Ah horizon (Rho = 0.91, $p < 0.001$) and the proportion of MAOM C (Rho = -0.67, $p < 0.01$) but no correlation with soil texture or MAOM in the Ahb horizon (Table 2).

Variability in mineralizable C in the Ah and Ahb horizons between sites was associated with differences in microbial communities. Specifically, potentially mineralizable C in the Ahb horizon was negatively correlated with total PLFA (Rho = -0.49, $p < 0.05$), total bacterial abundance (Rho = -0.50, $p < 0.05$) and GN bacterial abundance (Rho = -0.52, $p < 0.05$). Potentially mineralizable C in the Ah horizons also was negatively correlated with GN bacterial abundance (Rho = -0.64, $p < 0.01$) and positively correlated with the fungal to bacterial ratio (Rho = 0.52, $p < 0.05$).

3.2. *Thermodynamic efficiency*

Short term isothermal calorimetry assays revealed trends similar to the 100-day incubation in which Ahb horizons produced less CO_2 and also less heat (Table 4). Under basal respiration, CO_2 respiration and heat production were much higher in Ah horizon soils (Table 4), while little basal metabolism occurred in the Ahb horizon soils. However, Ahb horizons produced nearly 3.7 times more heat per unit of CO_2 (3105.6 ± 461.1 kJ mol^{-1} CO_2-C) than Ah horizons (841.1 ± 94.8 kJ mol^{-1} CO_2-C) (calorespirometric ratio; Table 4). The calorespirometric ratio was strongly correlated with soil texture (sand: Rho = -0.68, $p < 0.0001$; clay: Rho = 0.51, $p < 0.01$) when examined across Ah and Ahb horizons. The basal calorespirometric ratio strongly correlated with the proportion of MAOM C within both Ah and Ahb horizons (Ah: Rho = 0.79, $p < 0.0001$; Ahb: Rho = 0.74, $p < 0.001$). Basal heat production strongly correlated with the proportion of MAOM C within both Ahb horizons (Rho = 0.73, $p<0.001$) and Ah horizon (Rho = 0.70, $p<0.01$).

Following glucose addition, Ah horizons produced about 30% more heat (7.2 ± 0.12 J g^{-1} soil) than Ahb horizons (5.4 ± 0.38 J g^{-1} soil) and mineralized 1.5 times more CO_2 (168.7 ± 8.8 µg CO_2-C g^{-1} soil) than Ahb horizons (108.5 ±10.1 µg CO_2-C g^{-1} soil) (Table 4). There was a similar lag in heat production following glucose addition between the Ah and Ahb horizons in Swift Current and Cudworth soils (Fig. 4a; Fig. 4d) which represents a lag in microbial growth and metabolism. In contrast, Ahb soils from Gronlid metabolized the glucose more quickly than Ah horizons, while the opposite was true in soils from Bruno (Fig. 4e; Fig. 4c). Soils from St. Denis initially had a similar lag time in metabolism; however, one field replicate from the Ahb horizon consistently produced considerable heat between 30 and 45 hours after the start of the experiment (Fig. 4b). Ahb horizons also had higher calorespirometric ratios, producing significantly more heat per unit of CO_2 (697.8 ± 55.0 kJ mol^{-1} CO_2-C) than Ah horizons (627.0 ± 38.5 kJ mol^{-1} CO_2-C) following glucose addition. Further, Ahb horizons had a greater η_{eff} than Ah horizons (Table 4), although there may not have been full utilization of glucose in Ahb horizons from Bruno, St. Denis, and Cudworth.

4. Discussion

In this study we aimed to understand the mineralizability of SOC and the energetics of SOC and glucose use in erosion-buried C-rich horizons in soils with contrasting textures from different Chernozemic Soil Zones of Saskatchewan, Canada. We found that C-rich buried surface horizons contained less mineralizable SOC that dissipated less heat during both basal SOC and glucose metabolism. However, the calorespirometric ratio (heat dissipated per CO_2-C released) was on average more than two times greater during mineralization of indigenous SOC in buried horizon soils and was approximately 20% greater in soils amended with glucose in the Ahb horizons than in Ah horizons. In addition to these differences in C and energy use, we

observed that microbial abundance and community structure which differed under field conditions remained distinct after 100 days of incubation under controlled conditions. We propose that over decades of burial, limited fresh C input resulted in the co-development of energy-rich, but poorly available organic C along with a microbial community structure adapted to the deeper environment but also to the composition of highly recycled SOC that originated from the surface prior to burial.

4.1. Buried surface horizons contain predominantly stable SOC

Our observation of reduced biological availability of SOC in buried surface horizons is consistent with other studies on topsoil buried due to erosion (Doetterl et al., 2012; Wang et al., 2013; VandenBygaart et al., 2015). Although some size and density sorting can occur during hillslope transport (Gregorich et al., 1998; Doetterl et al., 2015), SOC composition of the erosion-deposited Ahb horizons would have been similar to a typical surface horizon at the time of burial, indicating that SOC persistence is derived from post-burial processes. Additionally, we do not know the concentration of SOC at burial, but it is likely some SOC has been lost over time, as it typical with microbial mineralization (Barros et al., 2024). The stability of the SOC present likely developed slowly over time (Schiedung et al., 2023) during the decades since the burial events occurred.

Carbon-rich buried surface horizons are distinct from typical subsoils because they were buried with C content and indigenous microbial communities that were characteristic of more resource-abundant surface soils. While typical subsoils have also been shown to mineralize a decreased proportion of SOC relative to topsoils (Salomé et al., 2010; Weiglein et al., 2022), this may be influenced by a greatly reduced microbial community abundance (Fierer et al., 2003; Eilers et al., 2012). Although we found that microbial abundance was positively correlated with

potentially mineralizable C, our findings show that despite a reduced microbial abundance in Ahb horizons, when mineralized C is normalized to total PLFA, Ahb horizons still produced significantly less CO_2-C than Ah horizons (Fig. 1b), suggesting that a reduced microbial abundance was not the primary factor in C persistence in Ahb horizons similar to findings by Su et al. (2023) who examined persistence of 5300-year old SOC.

Post-burial, the microbial communities in erosion-buried surface soils could continue to consume the C present in the Ahb horizon but would be limited by reduced fresh C input and environmental conditions deeper in the soil profile. The recycling of C-containing compounds from necromass is often energetically more favourable than synthesizing new monomers (Kästner et al., 2021; Wang and Kuzyakov, 2023), especially when extracellular enzymes are required. This is often observed in resource depleted environments, such as under years of bare fallow with no fresh C inputs (Nunan et al., 2015). With limited fresh C inputs, microorganisms in the Ahb horizons would experience an energy limitation after depleting the more readily available sources leading to increased reliance on recycling of C monomers from necromass. Further, as plant-derived C became increasingly depleted, there would be an accumulation of necromass if microorganisms did not recycle C monomers from necromass. As concentrations of microbial necromass are similar between Ah and Ahb horizons (Table 2), and limited change in microbial abundance when incubated in laboratory conditions in Ahb vs. Ah horizon, suggesting resource over environmental constraints, it is clear significant C recycling of microbial necromass is occurring in Ahb horizons. While current microbial abundance is considerably lower in Ahb horizons, this may have limited impact on microbial necromass concentrations which reflect longer-term past conditions (Liang et al., 2019). Helgason et al., (2014) examined the same soil profile at St. Denis as examined in this study and found greater abundance of PLFA

in Ahb horizons than Ah, suggesting that the ratio of microbial abundance may shift depending on the seasonal environment. Schiedung et al., (2023) performed deep soil flipping, burying the original surface horizon and showed while microbial biomass C decreased after burial, it did not linearly decrease with duration of burial. Further, bacterial necromass is often more intensively recycled than fungal necromass (Huang et al., 2020; Wang et al., 2021), possibly due to smaller C:N ratios (Deng and Liang, 2022), and despite similar contributions by bacteria to total microbial necromass (Huang et al., 2020), fungal necromass is 2.5 times greater in temperate ecosystems (Liang et al., 2019). Coupled with evidence that microbial necromass became the main source of C in volcanic buried surface soils (Hobara et al., 2020), this suggests that Ahb horizons in our study are more heavily reliant on microbially-derived C than Ah communities and is supported by our observation that despite significant microbial abundance, bacterial amino sugar C did not accumulate in the Ahb horizons (Table 2).

4.2. Co-development of persistent SOC and microbial communities over time after burial

Microbial communities are highly adaptable and therefore the active community structure often reflects the environmental conditions and resources present (Allison et al., 2005; Kramer et al., 2013). These temporal effects of resource availability can be realized in days or weeks (e.g. over the growing season) (Kramer et al., 2013) or after years of more slowly changing soil conditions (Allison et al., 2005). Despite development under nearly identical conditions between Ah vs. Ahb horizons prior to burial, microbial communities are distinctly different between the two soils (Table 2). Further, differences in microbial community abundance and structure between Ah and Ahb horizons in the field (Table 2) were maintained after 100-days of incubation under more optimal conditions of temperature and moisture in the lab (Fig. 2), suggesting at-depth environmental conditions do not account for differences in structure between

447 the two communities. Simon et al. (2024) found distinct microbial communities within
448 aggregates, coupled with distinct organic matter properties, which they suggest is a result of co-
449 development between resource and microbial communities. Further, a recent review by Philippot
450 et al. (2024) examining how microorganisms modify the soil habitat shows microorganisms
451 actively apply evolutionary processes in micro-habitats. Based on this, we propose that the
452 differences in Ahb vs. Ah communities is a reflection of continued community succession in
453 Ahb horizons following burial where fresh C inputs reduced, and readily available C became
454 limited as microorganisms decomposed the accessible SOC present, selecting for a microbial
455 community more adept at decomposing the new SOC profile.

456 Because GN bacteria are more reliant on labile C from plant litter and rhizodeposits, the
457 relative abundance of GN and GP bacteria can be used as a biomarker for C availability (Fanin et
458 al. 2019). This corresponds with the positive correlation between GN bacteria and the F:B ratio
459 with potentially mineralizable C that we observed in the Ah horizon, but which was not observed
460 in Ahb horizon soils where labile plant C had been depleted over time. When rhizodeposited C
461 enters the soil, it is first primarily consumed and held in GN bacterial and fungal biomass, before
462 eventually passing to GP bacteria and actinomycetes (Huang et al., 2020). Further, basal
463 incubation over the course of 588 days at 35°C and 60% water filled pore space showed an
464 increase in activation energy and a reduction in energy density (Plante et al., 2011). The
465 significantly larger GP:GN ratio observed between the Ahb vs Ah soils in the field (Table 2),
466 coupled with drastic changes in microbial abundance and composition in the Ah horizon but not
467 in the Ahb horizon supports a shift towards an increased reliance on more recycling of SOM-
468 derived C following burial of Ahb horizons. We propose that this co-development of microbial

community with resource conditions in the Ahb is analogous to the repeated decomposition of C in microbial hotspots typical of surface soils, such as within microaggregates.

4.3. Predominantly stable SOC in buried surface horizons led to higher calorespirometric ratios

Simultaneous measurement of CO_2-C mineralization and heat dissipated provides an index of the C and energy efficiency of SOM cycling (Harris et al., 2012). When heat dissipated is normalized to the amount of CO_2-C mineralized, the resulting calorespirometric ratio describes the C dynamics of the soil, elucidating links between microbial metabolism and the energy stored in the SOM (Barros et al., 2016). We propose that larger basal calorespirometric rations in Ahb horizon soils are a result of an increased proportion of persistent C coupled with a co-adapted microbial community. Specifically, we propose that there are two main mechanisms driving larger basal calorespirometric rations in Ahb horizon soils: i) surface-derived C has undergone significant microbial degradation, leading to more energy dense SOM with a higher thermal stability (Gunina and Kuzyakov, 2022) than SOM in the Ah horizon and, ii) Ahb horizons are more intensively recycling C, especially microbial necromass.

Buried surface horizons contain significantly more persistent C than Ah horizons (Fig. 1) and have larger basal calorespirometric ratios (Table 4). Increased C persistence is strongly correlated with increased thermal stability (Plante et al., 2011) which may provide more insight into the mechanistic basis driving the calorespirometric rations. A lower nominal oxidation state of C (NOSC), which requires more oxidation steps to be utilized (Gunina and Kuzyakov, 2022), and organo-mineral interactions (Gregorich et al., 2015), increase thermal stability, requiring a higher energy input by microorganisms to access. Microorganisms preferentially use more oxidized compounds such as carboxylic acids and amino acids (Barré et al., 2016; Keiluweit et

al., 2017; Gunina and Kuzyakov, 2022), with more reduced compounds like aromatics persisting longer in the soil (Jones et al., 2023), and evolving to a greater degree of reduction with increased mineralization (Barros et al, 2024), potentially leading to an accumulation of C with a lower NOSC in Ahb horizons. Calculations by Chakrawal et al. (2020) suggest the utilization of more reduced SOM, compared to less reduced SOM, will have larger calorespirometric ratios, especially if coupled with a high CUE by the microbial community. Further, there was a positive correlation between the proportion of MAOM C and the basal calorespirometric ratio (Rho = 0.78, $p < 0.0001$). The relationship between the proportion of MAOM C and basal calorespirometric ratios is even stronger when examined within each horizon separately (Ah: Rho = 0.79, $p < 0.0001$; Ahb: Rho = 0.74, $p < 0.001$). Accessing C compounds which requires a large energy input for microorganisms to access, such as MAOM, typically reduces EUE as additional steps required to breakdown the C increases the opportunity for energy loss (Wang and Kuzyakov, 2023). Differences in the calorespirometric ratio between the two horizons is likely strongly influenced by the proportion of C in organo-mineral bonds and energy density/availability of other SOM present, however further research examining the NSOC of the SOM is required.

Under resource-constrained conditions, microbial communities will often preferentially recycle C, such as amino sugars and other C monomers, which reduces the EUE of the microbial community (Wang and Kuzyakov, 2023). There was a strong positive correlation between the enrichment of bacterial and fungal necromass in SOC and the proportion of clay (Rho = 0.95, $p < 0.0001$; Rho = 0.73, $p < 0.001$), suggesting that mineral protection plays a role in protecting amino sugars from C recycling of necromass in Ahb horizons that warrants further exploration. Further, in the Ah horizon, we see a negative correlation between the enrichment of fungal

necromass and the proportion of clay (Rho = -0.49, $p < 0.05$), suggesting that when there is other more favourable C available, necromass may not be as intensively utilized and does not need to be protected by organo-mineral interactions to become enriched in soil. This intensive recycling of C may explain the larger calorespirometric ratios and reduced heat and CO_2 dissipation we observed in Ahb horizons compared to Ah horizons.

Potentially, differences in microbial metabolism may also account for variability in calorespirometric ratios between Ah and Ahb horizons. For examples, bacteria allocate more C to growth than fungi, and a narrower proportion of fungi to bacteria have better CUE (Soares and Rousk, 2019). We observed smaller fungal to bacterial ratios in Ahb horizons, suggesting an increased proportion of bacteria in the community, which may further exasperate differences in the calorespirometric ratios observed between Ah vs. Ahb soils. As the microbial community is a reflection of the resource and environmental conditions, this is also closely linked to the nature of the SOM. The nature of isothermal calorimetry experiments does not allow us to separate the impact of the microbial community vs. the impact of the SOC on our results (Barros et al., 2016).

Dynamics at the site of Gronlid were unique from the other soils, with very limited heat flow from the Ahb horizon (0.01 J g^{-1} soil), and even limited heat production in the Ah horizon (0.12 J g^{-1} soil), suggesting very limited, or a very low proportion of, energy releasing reactions occurred during the 48-hour incubation. Despite the limited heat production, significant CO_2 production still occurred, leading to very small calorespirometric ratios in the Ah (205.2 kJ mol^{-1} CO_2-C) and Ahb horizons (91.6 kJ mol^{-1} CO_2-C). This suggests that microbial metabolism was dominated by a greater proportion of energy-consuming anabolic reactions (Harris et al., 2012). Additionally, transitions in microbial physiological states, such as transitioning out of dormancy, or during maintenance processes such as regulating gene expression, etc. require significant

energy investments (Wang and Kuzyakov, 2023) and may explain the limited heat production despite significant CO_2 production at Gronlid. Limited research explores the balance of anabolic and catabolic reactions in soil under basal metabolism, especially of decomposition of highly persistent C. Further exploration of the nature of the C is needed to understand what is allowing for significant CO_2 production, despite limited heat production.

Substrate-induced calorespirometric ratios follow a similar trend to basal calorespirometric ratios, in which Ahb horizons produced more heat per CO_2 than Ah horizons (Table 4). Jones et al. (2018) demonstrated variability in CUE to the same added substrate between different communities, suggesting potentially a better CUE in Ahb horizons than Ah horizons. However, addition of glucose is known to cause priming of organic matter which has been shown to lead to variations in heat production (Arcand et al., 2017), and would be unsurprising to lead to calorespirometric ratios >469 kJ mol^{-1} CO_2-C (Chakrawal et al., 2021), the expected CR of complete utilization of glucose. Given the established differences in mineralizability of SOC in the Ahb and Ah horizons, co-metabolism of glucose and SOM (e.g. to mine N or P) in the Ahb would require higher activation energy, based on established links between SOM stability and thermal stability (Plante et al., 2011), leading to a lower EUE relative to CUE. Further, substrate-induced calorespirometric ratios at Gronlid were below the calorespirometric ratio of complete glucose utilization (>469 kJ mol^{-1} CO_2-C), unlike the other sites, suggsting a lack of organic matter priming. Similar to under basal metabolism, anabolic reactions by the microbial community may have consumed energy, partially offsetting additional heat released due to organic matter priming, however priming was not measured in this study. The differences between substrate-induced calorespirometric ratios between the Ah and Ahb horizons did not correlate with differences in the abundance or structure of the microbial community, or TOC,

suggesting that physical SOM properties, such as thermal stability and/ or energy density, may play a dominant role in the variability in the calorespirometric ratio, even under glucose amendment.

Ahb horizons were more thermodynamically efficient at utilizing glucose, based on the assumption that all glucose was completely metabolized in the 48-hour incubation (Table 4). While Bölscher et al. (2017) showed glucose had been almost completely utilized after 24-hours, Bölscher et al. (2016) also found variable utilization of glucose over 32-hours between soils with different land management histories, suggesting that due to potentially slow metabolism in Ahb horizons from some sites, glucose may not be fully utilized before the end of the assay. Our thermodynamic efficiencies were lower than values reported by studies which measured and adjusted for differences in glucose utilization (Bölscher et al., 2016, 2017). However, they are in-line with values reported by Harris et al. (2012) who showed that heat dissipation from surface soils significantly tapered off after ~30 hours. Thus, the differences in thermodynamic efficiency in Bruno, St. Denis, and Cudworth soils which still showed significant heat production near the end of the 48-hours may have been due to incomplete utilization of glucose rather than actual improved efficiency (Fig. 4). In soils from Gronlid and Swift Current, heat production tapered off similarly to Ah horizons, which means the observed increased thermodynamic efficiency may be reflective of a more efficient community.

4.4. *Soil texture and organo-mineral bonds has strong influence on SOC persistence in Ah but not Ahb horizons*

Site of origin accounted for as much variability in microbial community composition as horizon, indicating that both soil texture and edaphic factors play an important role in microbial community dynamics. Further, there was significant variation between C persistence at each site

584 within each horizon (Fig. 3). In the Ah horizon, C persistence strongly correlated with soil
585 texture. Sandier sites mineralized more CO_2 per unit SOC than heavier textured sites in Ah
586 horizons (Fig. 3a), and a greater proportion of MAOM C reduced potentially mineralizable C
587 (Rho = -0.67, $p < 0.01$), consistent with our current understanding that protection from microbial
588 decomposition by aggregation and organo-mineral bonds plays an important role in C persistence
589 (Salomé et al., 2010; Schrumpf et al., 2013; Jones et al., 2023; Su et al., 2023). Additionally,
590 basal heat correlated with proportion of MAOM C (Rho = 0.70, $p < 0.01$) suggesting organo-
591 mineral complexation also reduced the EUE of the microbial community. In the Ahb horizon
592 however, soil texture and the proportion of MAOM C had no correlation with C persistence,
593 although the proportion of MAOM C strongly correlated with basal heat production (Rho = 0.73,
594 $p < 0.001$). This suggests that while breaking of organo-mineral bonds to access C reduced the
595 EUE of the microbial community, it is not the main mechanisms driving C persistence in Ahb
596 horizons, unlike in Ah horizons. Repeated, long-term decomposition coupled with minimal new
597 C inputs may have left energetically unfavorable C remaining in the Ahb horizon, which is
598 further exasperated by organo-mineral bonds and a lack of easily biodegradable C, coupled with
599 a co-adapted microbial community, may be more strongly driving C persistence than the
600 aggregation and organo-mineral bonds driving C persistence in Ah horizons.

601 How organic matter decomposition proceeds can shift depending on the stage of
602 decomposition, incoming fresh resources, environmental conditions and the decomposer
603 community composition (Kaiser et al., 2014; Lehmann and Kleber, 2015; Xue et al., 2024). For
604 example, during initial stages of decomposition, the NOSC consistently decreases, but during
605 intermediate stages of decomposition, the NOSC can either increase or decrease depending on
606 the rate of decomposition, soil properties, and initial composition of the litter (Wang &

607 Kuzyakov, 2023). In a typical surface soil that receives frequent C inputs, SOM is a mixture of
608 compounds that span a wide range of decomposition, making it challenging to measure distinct
609 pools of persistent C and readily biodegradable C. Further, the majority of C turnover is believed
610 to occur in microbial hotspots (Kuzyakov and Blagodatskaya, 2015) that are most readily
611 identified using C tracing techniques and are typically only studied during initial stages of C
612 turnover (Huang et al., 2020; Lange et al., 2024). Examination of micro-aggregates, a common
613 example of a microbial hotspot, has found distinct SOM and microbial community composition
614 which likely co-developed together (Simon et al., 2024), however in too small of volumes to
615 examine C mineralization or energetics of microbial decomposition. Alternatively, large volume
616 C-rich buried surface horizons also undergo repeated microbial decomposition following burial
617 and contain a large proportion of persistent C (Fig. 1), which gave us the opportunity to examine
618 the dynamics of microbial decomposition of a "later-stage" microbial hotspot.

619 **5. Conclusion**

620 Consistent with our hypothesis that SOC in Ahb horizons was more resistant to
621 mineralization to CO_2 than Ah horizons, regardless of the soil texture, the lack of correlation
622 between clay content and potentially mineralizable C in Ahb horizons suggests that C stability is
623 primarily due to repeated microbial decomposition rather than physical stabilization in
624 aggregates or on mineral surfaces. The lower CO_2 respiration and heat dissipation as well as
625 larger calorespirometric ratio by microbial communities in Ahb compared to Ah soils reflects C
626 and energetic limitations. The limited increase in CO_2 respiration from the addition of glucose,
627 coupled with minimal change in microbial community during incubation under laboratory
628 conditions in Ahb soils suggests that exposure to surface conditions may not destabilize the C in
629 Ahb horizons. However, greater plant C inputs at or near the surface could shift the microbial

community structure and potentially help to overcome the energetic limitations to using the C in Ahb soils. With increasing interest in translocating soil from depositional areas to eroded knolls to improve crop productivity (e.g. Schneider et al., 2021), buried surface horizons may be re-exposed to surface conditions, showing the need for a better understanding of the persistence of the significant stores of C remaining in buried surface soils prior to excavation. Further investigation into the energy density and availability of SOM after decades of burial, coupled with a more in-depth investigation into the active microbial community structure could strengthen our understanding of C cycling where SOM is dominated by persistent SOC.

Acknowledgments

The authors wish to thank Jesse Reimer for technical assistance, the Natural Sciences and Engineering Research Council of Canada and the Global Institute for Food Security for funding, and the St. Denis National Wildlife Area (SDNWA) and partnering producers for access to their field sites. The authors also wish to think Adam Gillespie for his insightful feedback on this manuscript.

References

Alcántara, V., Don, A., Vesterdal, L., Well, R., Nieder, R., 2017. Stability of buried carbon in deep-ploughed forest and cropland soils - implications for carbon stocks. Scientific Reports 7, 5511. doi:10.1038/s41598-017-05501-y

Allison, V., Miller, R., Jastrow, J., Matamala, R., Zak, D., 2005. Changes in Soil Microbial Community Structure in a Tallgrass Prairie Chronosequence. Soil Science Society of America Journal 69, 1412–1421. doi:10.2136/sssaj2004.0252

Appuhn, A., Joergensen, R.G., 2006. Microbial colonisation of roots as a function of plant species. Soil Biology & Biochemistry 38, 1040–1051.

Arcand, M.M., Levy-Booth, D.J., Helgason, B.L., 2017. Resource Legacies of Organic and Conventional Management Differentiate Soil Microbial Carbon Use. Frontiers in Microbiology 8, 2293. doi:10.3389/fmicb.2017.02293

Barré, P., Plante, A.F., Cécillon, L., Lutfalla, S., Baudin, F., Bernard, S., Christensen, B.T., Eglin, T., Fernandez, J.M., Houot, S., Kätterer, T., Le Guillou, C., Macdonald, A., van Oort, F., Chenu, C., 2016. The energetic and chemical signatures of persistent soil organic matter. Biogeochemistry 130, 1–12. doi:10.1007/s10533-016-0246-0

Barros, N., Hansen, L.D., Piñeiro, V., Pérez-Cruzado, C., Villanueva, M., Proupín, J., Rodríguez-Añón, J.A., 2016. Factors influencing the calorespirometric ratios of soil microbial metabolism. Soil Biology and Biochemistry 92, 221–229. doi:10.1016/j.soilbio.2015.10.007

Barros, N., Popovic, M., Molina-Valero, J., Lestido-Cardama, Y., Pérez-Cruzado, C., 2024. Unravelling the thermodynamic properties of soil ecosystems in mature beech forests. Scientific Reports 14, 16644. doi:10.1038/s41598-024-67590-w

Berhe, A.A., Harden, J.W., Torn, M.S., Harte, J., 2008. Linking soil organic matter dynamics and erosion-induced terrestrial carbon sequestration at different landform positions. Journal of Geophysical Research: Biogeosciences 113, 2008JG000751. doi:10.1029/2008JG000751

Bölscher, T., Paterson, E., Freitag, T., Thornton, B., Herrmann, A.M., 2017. Temperature sensitivity of substrate-use efficiency can result from altered microbial physiology without change to community composition. Soil Biology and Biochemistry 109, 59–69. doi:10.1016/j.soilbio.2017.02.005

Bölscher, T., Wadsö, L., Börjesson, G., Herrmann, A.M., 2016. Differences in substrate use efficiency: impacts of microbial community composition, land use management, and substrate complexity. Biology and Fertility of Soils 52, 547–559. doi:10.1007/s00374-016-1097-5

Cambardella, C.A., Elliott, E.T., 1992. Particulate Soil Organic-Matter Changes across a Grassland Cultivation Sequence. Soil Science Society of America Journal 56, 777–783.

Chakrawal, A., Herrmann, A.M., Manzoni, S., 2021. Leveraging energy flows to quantify microbial traits in soils. Soil Biology and Biochemistry 155, 108169. doi:10.1016/j.soilbio.2021.108169

Chakrawal, A., Herrmann, A.M., Šantrůčková, H., Manzoni, S., 2020. Quantifying microbial metabolism in soils using calorespirometry — A bioenergetics perspective. Soil Biology and Biochemistry 148, 107945. doi:10.1016/j.soilbio.2020.107945

Chaopricha, N.T., Marín-Spiotta, E., 2014. Soil burial contributes to deep soil organic carbon storage. Soil Biology and Biochemistry 69, 251–264. doi:10.1016/j.soilbio.2013.11.011

Deng, F., Liang, C., 2022. Revisiting the quantitative contribution of microbial necromass to soil carbon pool: Stoichiometric control by microbes and soil. Soil Biology and Biochemistry 165, 108486. doi:10.1016/j.soilbio.2021.108486

Doetterl, S., Cornelis, J.-T., Six, J., Bodé, S., Opfergelt, S., Boeckx, P., Van Oost, K., 2015. Soil redistribution and weathering controlling the fate of geochemical and physical carbon stabilization mechanisms in soils of an eroding landscape. Biogeosciences 12, 1357–1371. doi:10.5194/bg-12-1357-2015

Doetterl, S., Six, J., Van Wesemael, B., Van Oost, K., 2012. Carbon cycling in eroding landscapes: geomorphic controls on soil organic C pool composition and C stabilization. Global Change Biology 18, 2218–2232. doi:10.1111/j.1365-2486.2012.02680.x

Eilers, K.G., Debenport, S., Anderson, S., Fierer, N., 2012. Digging deeper to find unique microbial communities: The strong effect of depth on the structure of bacterial and archaeal communities in soil. Soil Biology and Biochemistry 50, 58–65. doi:10.1016/j.soilbio.2012.03.011

Ellis, S., Ritz, K., 2018. A modified high-throughput analysis of PLFAs in soil. MethodsX 5, 1491–1497. doi:10.1016/j.mex.2018.10.022

Engelking, B., Flessa, H., Joergensen, R.G., 2007. Shifts in amino sugar and ergosterol contents after addition of sucrose and cellulose to soil. Soil Biology & Biochemistry 39, 2111–2118.

Fierer, N., Schimel, J.P., Holden, P.A., 2003. Variations in microbial community composition through two soil depth profiles. Soil Biology and Biochemistry 35, 167–176. doi:10.1016/S0038-0717(02)00251-1

Gregorich, E.G., Gillespie, A.W., Beare, M.H., Curtin, D., Sanei, H., Yanni, S.F., 2015. Evaluating biodegradability of soil organic matter by its thermal stability and chemical composition. Soil Biology and Biochemistry 91, 182–191. doi:10.1016/j.soilbio.2015.08.032

Gregorich, E.G., Greer, K.J., Anderson, D.W., Liang, B.C., 1998. Carbon distribution and losses: erosion and deposition effects. Soil and Tillage Research 47, 291–302. doi:10.1016/S0167-1987(98)00117-2

Gunina, A., Kuzyakov, Y., 2022. From energy to (soil organic) matter. Global Change Biology 28, 2169–2182. doi:10.1111/gcb.16071

Haddix, M.L., Gregorich, E.G., Helgason, B.L., Janzen, H., Ellert, B.H., Francesca Cotrufo, M., 2020. Climate, carbon content, and soil texture control the independent formation and persistence of particulate and mineral-associated organic matter in soil. Geoderma 363, 114160. https://doi.org/10.1016/j.geoderma.2019.114160

Harris, J.A., Ritz, K., Coucheney, E., Grice, S.M., Lerch, T.Z., Pawlett, M., Herrmann, A.M., 2012. The thermodynamic efficiency of soil microbial communities subject to long-term stress is lower than those under conventional input regimes. Soil Biology and Biochemistry 47, 149–157. doi:10.1016/j.soilbio.2011.12.017

Helgason, B.L., Konschuh, H.J., Bedard-Haughn, A., VandenBygaart, A.J., 2014. Microbial distribution in an eroded landscape: Buried A horizons support abundant and unique communities. Agriculture, Ecosystems & Environment 196, 94–102. doi:10.1016/j.agee.2014.06.029

Helgason, B.L., Walley, F.L., Germida, J.J., 2010. No-till soil management increases microbial biomass and alters community profiles in soil aggregates. Applied Soil Ecology 46, 390–397. doi:10.1016/j.apsoil.2010.10.002

Hendershot, W.H., Lalonde, H, Duquette, M, 2008. Soil reaction and exchangeable acidity, in: Carter, M.R., Gregorich, E.G. (Eds.), Soil Sampling and Methods of Analysis. CRC Press, Boca Ration, FL, pp. 173–178.

Herrmann, A.M., Coucheney, E., Nunan, N., 2014. Isothermal Microcalorimetry Provides New Insight into Terrestrial Carbon Cycling. Environmental Science & Technology 48, 4344–4352. doi:10.1021/es403941h

Hobara, S., Ogawa, H., Benner, R., 2020. Amino acids and amino sugars as molecular indicators of the origins and alterations of organic matter in buried tephra layers. Geoderma 373, 114449. doi:10.1016/j.geoderma.2020.114449

Huang, J., Liu, W., Deng, M., Wang, X., Wang, Z., Yang, L., Liu, L., 2020. Allocation and turnover of rhizodeposited carbon in different soil microbial groups. Soil Biology and Biochemistry 150, 107973. doi:10.1016/j.soilbio.2020.107973

Indorf, C., Dyckmans, J., Khan, K.S., Joergensen, R.G., 2011. Optimisation of amino sugar quantification by HPLC in soil and plant hydrolysates. Biology and Fertility of Soils 47, 387–396. doi:10.1007/s00374-011-0545-5

Joergensen, R.G., 2018. Amino sugars as specific indices for fungal and bacterial residues in soil. Biology and Fertility of Soils 54, 559–568.

Jones, A.R., Dalal, R.C., Gupta, V.V.S.R., Schmidt, S., Allen, D.E., Jacobsen, G.E., Bird, M., Grandy, A.S., Sanderman, J., 2023. Molecular complexity and diversity of persistent soil organic matter. Soil Biology and Biochemistry 184, 109061. doi:10.1016/j.soilbio.2023.109061

Jones, D.L., Hill, P.W., Smith, A.R., Farrell, M., Ge, T., Banning, N.C., Murphy, D.V., 2018. Role of substrate supply on microbial carbon use efficiency and its role in interpreting soil microbial community-level physiological profiles (CLPP). Soil Biology and Biochemistry 123, 1–6. doi:10.1016/j.soilbio.2018.04.014

Kaiser, C., Franklin, O., Dieckmann, U., Richter, A., 2014. Microbial community dynamics alleviate stoichiometric constraints during litter decay. Ecology Letters 17, 680–690. doi:10.1111/ele.12269

Kästner, M., Miltner, A., Thiele-Bruhn, S., Liang, C., 2021. Microbial Necromass in Soils—Linking Microbes to Soil Processes and Carbon Turnover. Frontiers in Environmental Science 9. doi:10.3389/fenvs.2021.756378

Keiluweit, M., Wanzek, T., Kleber, M., Nico, P., Fendorf, S., 2017. Anaerobic microsites have an unaccounted role in soil carbon stabilization. Nature Communications 8, 1771. doi:10.1038/s41467-017-01406-6

Kögel-Knabner, I., Guggenberger, G., Kleber, M., Kandeler, E., Kalbitz, K., Scheu, S., Eusterhues, K., Leinweber, P., 2008. Organo-mineral associations in temperate soils: Integrating biology, mineralogy, and organic matter chemistry. Journal of Plant Nutrition and Soil Science 171, 61–82. doi:10.1002/jpln.200700048

Kramer, S., Marhan, S., Haslwimmer, H., Ruess, L., Kandeler, E., 2013. Temporal variation in surface and subsoil abundance and function of the soil microbial community in an arable soil. Soil Biology and Biochemistry 61, 76–85. doi:10.1016/j.soilbio.2013.02.006

Kroetsch, D., Wang, C., 2008. Particle Size Distrubtion, in: Carter, M.R., Gregorich, E.G. (Eds.), Soil Sampling and Methods of Analysis. CRC Press, Boca Ration, FL, pp. 713–725.

Kuzyakov, Y., Blagodatskaya, E., 2015. Microbial hotspots and hot moments in soil: Concept & review. Soil Biology and Biochemistry 83, 184–199. doi:10.1016/j.soilbio.2015.01.025

Lange, M., Azizi-Rad, M., Dittmann, G., Lange, D.F., Orme, A.M., Schroeter, S.A., Simon, C., Gleixner, G., 2024. Stability and carbon uptake of the soil microbial community is determined by differences between rhizosphere and bulk soil. Soil Biology and Biochemistry 189, 109280. doi:10.1016/j.soilbio.2023.109280

Lehmann, J., Kleber, M., 2015. The contentious nature of soil organic matter. Nature 528, 60–68. doi:10.1038/nature16069

Lehmann, J., Hansel, C.M., Kaiser, C., Kleber, M., Maher, K., Manzoni, S., Nunan, N., Reichstein, M., Schimel, J.P., Torn, M.S., Wieder, W.R., Kögel-Knabner, I., 2020. Persistence of soil organic carbon caused by functional complexity. Nature Geoscience 13, 529–534. doi:10.1038/s41561-020-0612-3

Liang, C., Amelung, W., Lehmann, J., Kästner, M., 2019. Quantitative assessment of microbial necromass contribution to soil organic matter. Global Change Biology 25, 3578–3590. doi:10.1111/gcb.14781

Nunan, N., Lerch, T.Z., Pouteau, V., Mora, P., Changey, F., Kätterer, T., Giusti-Miller, S., Herrmann, A.M., 2015. Metabolising old soil carbon: Simply a matter of simple organic matter? Soil Biology and Biochemistry 88, 128–136. doi:10.1016/j.soilbio.2015.05.018

Oksanen, J., Simpson, G. L., Guillaume, B., Kindt, R., Legendre, P., Minchin, P. R., O'Hara, R.B., Solymos, P., Stevens, M. H. H., Szoecs, E., Wagner, J., Barbour, M., Bedward, M. Bolker, B., Borcard, D., Carvalho, G., Chirico, M., De Cacares, M., Durand, S., … Weedin, J. (2022). vegan: Community Ecology Package. R Package Version 2.6-4. Available at: https://cran.r-project.org/package=vegan

Philippot, L., Chenu, C., Kappler, A., Rillig, M.C., Fierer, N., 2024. The interplay between microbial communities and soil properties. Nature Reviews Microbiology 22, 226–239. doi:10.1038/s41579-023-00980-5

Plante, A.F., Fernández, J.M., Haddix, M.L., Steinweg, J.M., Conant, R.T., 2011. Biological, chemical and thermal indices of soil organic matter stability in four grassland soils. Soil Biology and Biochemistry 43, 1051–1058. doi:10.1016/j.soilbio.2011.01.024

Salomé, C., Nunan, N., Pouteau, V., Lerch, T.Z., Chenu, C., 2010. Carbon dynamics in topsoil and in subsoil may be controlled by different regulatory mechanisms. Global Change Biology 16, 416–426. doi:10.1111/j.1365-2486.2009.01884.x

Schiedung, M., Don, A., Beare, M.H., Abiven, S., 2023. Soil carbon losses due to priming moderated by adaptation and legacy effects. Nature Geoscience 16, 909–914. doi:10.1038/s41561-023-01275-3

Schneider, S.K., Cavers, C.G., Duke, S.E., Schumacher, J.A., Schumacher, T.E., Lobb, D.A., 2021. Crop responses to topsoil replacement within eroded landscapes. Agronomy Journal 113, 2938–2949. doi:10.1002/agj2.20635

Schrumpf, M., Kaiser, K., Guggenberger, G., Persson, T., Kögel-Knabner, I., Schulze, E.-D., 2013. Storage and stability of organic carbon in soils as related to depth, occlusion within aggregates, and attachment to minerals. Biogeosciences 10, 1675–1691. doi:10.5194/bg-10-1675-2013

Simon, E., Guseva, K., Darcy, S., Alteio, L., Pjevac, P., Schmidt, H., Jenab, K., Ranits, C., Kaiser, C., 2024. Distinct microbial communities are linked to organic matter properties in millimetre-sized soil aggregates. The ISME Journal 18, wrae156. doi:10.1093/ismejo/wrae156

Skjemstad, J.O., Baldock, J., 2008. Total and Organic Carbon, in: Carter, M.R., Gregorich, E.G. (Eds.), Soil Sampling and Methods of Analysis. CRC Press, Boca Ration, FL, pp. 225–237.

Su, J., Zhang, H., Han, X., Lv, R., Liu, L., Jiang, Y., Li, H., Kuzyakov, Y., Wei, C., 2023. 5300-Year-old soil carbon is less primed than young soil organic matter. Global Change Biology 29, 260–275. doi:10.1111/gcb.16463

TA Instruments (2012). TAM Air Getting Started Guide. New Castle, DE: TA Instruments.

Van Oost, K., Govers, G., Quine, T.A., Heckrath, G., Olesen, J.E., De Gryze, S., Merckx, R., 2005. Landscape-scale modeling of carbon cycling under the impact of soil redistribution: The role of tillage erosion. Global Biogeochemical Cycles 19, 2005GB002471. doi:10.1029/2005GB002471

VandenBygaart, A.J., Gregorich, E.G., Helgason, B.L., 2015. Cropland C erosion and burial: Is buried soil organic matter biodegradable? Geoderma 239–240, 240–249. doi:10.1016/j.geoderma.2014.10.011

VandenBygaart, A.J., Kroetsch, D., Gregorich, E.G., Lobb, D., 2012. Soil C eroion and burial in cropland. Global Change Biology 18, 1441–1452. doi:10.1111/j.1365-2486.2011.02604.x

Wang, B., An, S., Liang, C., Liu, Y., Kuzyakov, Y., 2021. Microbial necromass as the source of soil organic carbon in global ecosystems. Soil Biology and Biochemistry 162, 108422. doi:10.1016/j.soilbio.2021.108422

Wang, C., Kuzyakov, Y., 2023. Energy use efficiency of soil microorganisms: Driven by carbon recycling and reduction. Global Change Biology 29, 6170–6187. doi:10.1111/gcb.16925

Wang, X., Cammeraat, E.L.H., Cerli, C., Kalbitz, K., 2014. Soil aggregation and the stabilization of organic carbon as affected by erosion and deposition. Soil Biology and Biochemistry 72, 55–65. doi:10.1016/j.soilbio.2014.01.018

Wang, X., Cammeraat, L.H., Wang, Z., Zhou, J., Govers, G., Kalbitz, K., 2013. Stability of organic matter in soils of the Belgian Loess Belt upon erosion and deposition. European Journal of Soil Science 64, 219–228. doi:10.1111/ejss.12018

Wang, Z., Van Oost, K., Lang, A., Quine, T., Clymans, W., Merckx, R., Notebaert, B., Govers, G., 2014. The fate of buried organic carbon in colluvial soils: a long-term perspective. Biogeosciences 11, 873–883. doi:10.5194/bg-11-873-2014

Weiglein, T.L., Strahm, B.D., Bowman, M.M., Gallo, A.C., Hatten, J.A., Heckman, K.A., Matosziuk, L.M., Nave, L.E., Possinger, A.R., SanClements, M.D., Swanston, C.W., 2022. Key predictors of soil organic matter vulnerability to mineralization differ with depth at a continental scale. Biogeochemistry 157, 87–107. doi:10.1007/s10533-021-00856-x

Wixon, D.L., Balser, T.C., 2013. Toward conceptual clarity: PLFA in warmed soils. Soil Biology and Biochemistry 57, 769–774. doi:10.1016/j.soilbio.2012.08.016

Xue, Z., Qu, T., Li, X., Chen, Q., Zhou, Z., Wang, B., Lv, X., 2024. Different contributing processes in bacterial vs. fungal necromass affect soil carbon fractions during plant residue transformation. Plant and Soil 494, 301–319. doi:10.1007/s11104-023-06277-z

Table 1. Ecoregion, current vegetation and soil zone and classification of Swift Current, St. Denis National Wildlife Area (St. Denis), Bruno, Cudworth and Gronlid.

Site	Ecoregion	Current Vegetation	Soil Zone	Soil Classification IUSS/ CSSS[a]
Swift Current	Mixed Grassland	Annual Cropland	Brown	Haplic Kastanozem/ Orthic Brown Chernozem
St. Denis	Mixed Moist Grassland	Grassland	Dark Brown	Haplic Kastanozem/ Orthic Dark Brown Chernozem
Bruno	Mixed Moist Grassland	Annual Cropland	Dark Brown	Haplic Kastanozem/ Orthic Dark Brown Chernozem
Cudworth	Aspen Parkland	Annual Cropland	Black	Chernozem/ Orthic Black Chernozem
Gronlid	Boreal Transition	Annual Cropland	Dark Grey	Greyzem/ Orthic Dark Grey Chernozem

[a]IUSS- International Union of Soil Science; CSSS- Canadian Soil Science Society

Table 2. Soil texture, soil organic C (SOC), pH, bacterial C, and fungal concentrations, microbial properties, and proportion of mineral associated organic matter (MAOM) from field samples collected from the surface (Ah) and buried surface (Ahb) horizons from five sites across Saskatchewan.

Site	Horizon	% Clay	% Sand	SOC (mg OC g^{-1} soil)	pH	Bacterial necromass C (mg C g^{-1} SOC)	Fungal necromass C (mg C g^{-1} SOC)	Total PLFA (nmol g^{-1} soil)	GP.GN	F.B	MAOM (mg MAOM C g^{-1} SOC)
All sites	Ah	NA	NA	30.9 ± 2.05 A	NA	41.0 ± 1.78 A	95.4 ± 3.92 A	77.2 ± 8.94 A	0.64 ± 0.019 B	0.056 ± 0.0036 A	710 ± 1.8 B
	Ahb	NA	NA	25.6 ± 2.90 A	NA	31.7 ± 2.78 B	103.7 ± 6.27 A	26.8 ± 2.18 B	0.84 ± 0.023 A	0.021 ± 0.0019 B	793 ± 1.8 A
Swift	Ah	17	43	32.2 ± 1.50 a	6.1	40.2 ± 1.46 a	110.2 ± 5.73 a	54.6 ± 4.36 a	0.59 ± 0.013 b	0.066 ± 0.0079 a	821 ± 0.5 b
Current	Ahb	17	45	12.1 ± 0.10 b	7.3	36.7 ± 1.12 a	139.2 ± 11.22 a	17.3 ± 2.72 b	0.83 ± 0.008 a	0.022 ± 0.0014 b	883 ± 1.2 a
St. Denis	Ah	23	47	29.8 ± 1.50 a	7.8	49.3 ± 4.34 a	98.3 ± 7.72 a	84.4 ± 6.77 a	0.69 ± 0.021 b	0.041 ± 0.0053 a	711 ± 3.1 a
	Ahb	17	51	42.6 ± 7.77 a	7.7	32.4 ± 4.60 b	110.1 ± 9.47 a	36.2 ± 7.03 b	0.98 ± 0.006 a	0.023 ± 0.0079 a	783 ± 0.2 a
Bruno	Ah	35	39	46.5 ± 0.82 a	7.7	45.6 ± 1.18 a	68.4 ± 5.65 b	93.0 ± 6.54 a	0.55 ± 0.014 b	0.046 ± 0.0024 a	752 ± 1.0 b
	Ahb	43	35	21.5 ± 1.12 b	7.5	49.4 ± 3.50 a	114.9 ± 7.44 a	27.3 ± 3.06 b	0.78 ± 0.055 a	0.026 ± 0.0018 b	848 ± 2.6 a
Cudworth	Ah	13	63	25.2 ± 1.14 a	7.6	42.8 ± 1.78 a	95.4 ± 1.27 a	87.2 ± 7.32 a	0.60 ± 0.002 b	0.057 ± 0.0032 a	640 ± 1.3 b
	Ahb	15	55	21.3 ± 0.64 a	7.7	22.8 ± 0.68 b	78.0 ± 3.37 b	28.3 ± 2.69 b	0.72 ± 0.027 a	0.018 ± 0.0020 b	739 ± 1.8 a
Gronlid	Ah	19	57	20.8 ± 0.33 b	5.0	29.8 ± 1.60 a	104.8 ± 3.80 a	66.8 ± 8.75 a	0.77 ± 0.026 b	0.067 ± 0.0109 a	627 ± 2.6 a
	Ahb	9	61	26.0 ± 0.66 a	7.0	17.4 ± 1.05 b	76.0 ± 3.28 b	24.6 ± 0.30 b	0.85 ± 0.012 a	0.014 ± 0.0012 b	708 ± 2.5 a

Letters represent significant differences at $p<0.05$. Capital letters indicate differences between horizons, uncapitalized letters represent significant differences between horizons within each site. Values represent the mean ± 1 SE.

Table 3. Proportional change in Total PLFA (nmol g^{-1} soil) , Gram positive (GP) bacteria (mol %), Gram negative (GN) bacteria (mol %), total bacterial (mol %) and fungal (mol %) biomarkers between field samples and after 100-days of incubation, proportional to field communities.

Site	Horizon	Total PLFA	GP	GN	GP.GN	Bacteria	Fungi	FB
		(% change)						
All sites	Ah	- 42.0 ± 2.97A	27.0 ± 3.09A	- 2.03 ± 1.49A	30.6 ± 2.81 A	20.9 ± 2.78 B	- 37.0 ± 4.40 A	- 46.2 ± 3.95 A
	Ahb	- 19.4 ± 4.54B	11.5 ± 2.49B	- 5.27 ± 1.06A	17.7 ± 2.52 B	11.7 ± 1.68 A	- 6.3 ± 6.10 B	- 18.0 ± 5.24 B
Swift	Ah	- 38.2 ± 4.96 a	29.2 ± 4.28 a	- 5.06 ± 0.67 a	36.2 ± 5.34 a	20.5 ± 1.51 b	- 30.7 ± 2.54 a	- 42.4 ± 2.65 a
Current	Ahb	- 15.7 ± 4.67 b	11.0 ± 2.62 b	- 9.18 ± 0.99 b	22.3 ± 3.89 a	16.6 ± 0.54 a	- 3.5 ± 8.81 b	- 17.2 ± 7.66 b
St. Denis	Ah	- 43.7 ± 2.80 a	26.4 ± 7.84 a	- 6.59 ± 0.32 a	34.0 ± 9.37 a	15.5 ± 0.81 b	- 32.0 ± 17.35 a	- 41.2 ± 15.04 a
	Ahb	5.6 ± 15.25 b	3.5 ± 0.94 b	- 2.13 ± 1.68 a	4.2 ± 1.39 b	1.4 ± 0.79 a	- 51.7 ± 0.57 a	- 54.9 ± 2.23 a
Bruno	Ah	- 25.3 ± 5.50 a	17.2 ± 2.01 a	- 2.37 ± 1.09 a	20.1 ± 2.26 a	14.4 ± 0.52 b	- 50.9 ± 6.07 a	- 56.0 ± 5.00 a
	Ahb	- 24.8 ± 5.23 a	13.5 ± 6.66 a	- 1.68 ± 0.19 a	16.5 ± 7.81 a	18.3 ± 0.46 a	11.4 ± 2.61 b	- 5.9 ± 1.92 b
Cudworth	Ah	- 43.7 ± 1.03 a	15.9 ± 2.46 a	- 4.20 ± 0.97 a	23.7 ± 0.50 a	12.1 ± 0.59 a	- 29.3 ± 6.66 a	- 36.1 ± 5.94 a
	Ahb	- 33.5 ± 7.23 a	18.9 ± 8.75 a	- 4.49 ± 3.17 a	24.1 ± 5.34 a	13.1 ± 1.18 a	- 5.1 ± 3.16 b	- 19.4 ± 5.54 a
Gronlid	Ah	- 55.2 ± 5.92 a	46.4 ± 3.58 a	6.95 ± 4.86 a	37.5 ± 5.04 a	43.9 ± 0.65 a	- 43.9 ± 9.78 a	- 58.4 ± 8.19 a
	Ahb	- 28.5 ± 1.71 b	8.8 ± 3.24 b	- 7.96 ± 1.93 b	18.2 ± 2.86 b	8.1 ± 3.24 a	6.7 ± 14.69 b	- 1.5 ± 12.79 b

Letters represent significant differences at $p<0.05$. Capital letters indicate differences between horizons, uncapitalized letters represent significant differences between horizons within each site. Values represent the mean ± 1 SE.

Table 4. Thermodynamic properties of buried surface horizons compared to surface horizons under short-term (48-hour) incubation with and without the addition of glucose.

Site	Horizon	Basal Soil			Glucose Amended			
		Respiration (μg CO_2-C g^{-1} soil)	Heat (J g^{-1} soil)	Caloresp. Ratio (kJ mol^{-1} CO_2-C)	Respiration (μg CO_2-C g^{-1} soil)	Heat (J g^{-1} soil)	Caloresp. Ratio (kJ mol^{-1} CO_2-C)	η_{eff} †
All sites	Ah	16.9 ± 1.1 A	1.34 ± 0.21 A	841.1 ± 94.8 B	168.7 ± 8.8 A	7.2 ± 0.12 A	627.0 ± 38.5 B	0.64 ± 0.006 B
	Ahb	1.9 ± 0.3 B	0.40 ± 0.08 B	3105.6 ± 461.3 A	108.5 ±10.1 B	5.4 ± 0.38 B	697.8 ± 55.0 A	0.72 ± 0.019 A
Swift	Ah	17.3 ± 1.1 a	1.36 ± 0.06 a	893.6 ± 12.5 b	218.3 ± 19.5 a	7.4 ± 0.31 a	775.5 ± 119.6 b	0.63 ± 0.017 a
Current	Ahb	1.3 ± 0.4 b	0.65 ± 0.04 b	4233.2 ± 250.4 a	68.5 ± 19.5 b	3.4 ± 0.34 b	950.0 ± 211.6 a	0.83 ± 0.017 b
St. Denis	Ah	15.9 ± 1.8 a	1.35 ± 0.12 a	1049.0 ± 68.3 b	144.6 ± 1.0 a	6.5 ± 0.04 a	649.8 ± 16.2 b	0.67 ± 0.003 a
	Ahb	3.7 ± 1.2 b	0.49 ± 0.14 b	1463.5 ± 46.9 a	69.8 ± 19.9 b	5.3 ± 1.24 a	780.0 ± 67.7 a	0.73 ± 0.205 a
Bruno	Ah	25.8 ± 4.5 a	2.31 ± 0.12 a	1337.3 ± 128.3 b	148.3 ± 4.5 a	7.1 ± 0.23 a	769.2 ± 5.5 a	0.64 ± 0.013 b
	Ahb	1.9 ± 0.0 b	0.78 ± 0.08 b	4569.7 ± 321.0 a	119.1 ± 3.5 b	6.1 ± 0.24 b	695.2 ± 17.8 a	0.69 ± 0.012 a
Cudworth	Ah	19.7 ± 1.1 a	1.14 ± 0.10 a	733.7 ± 91.4 a	176.9 ± 6.2 a	7.1 ± 0.07 a	566.2 ± 17.3 b	0.63 ± 0.005 a
	Ahb	1.0 ± 0.1 b	0.09 ± 0.08 b	3677.2 ± 1508.5 a	137.9 ± 1.9 b	7.3 ± 0.12 a	600.6 ± 32.4 a	0.63 ± 0.006 a
Gronlid	Ah	11.2 ± 3.4 a	0.12 ± 0.04 a	205.2 ± 63.3 a	227.4 ± 7.8 a	7.6 ± 0.20 a	410.0 ± 10.6 b	0.61 ± 0.010 b
	Ahb	1.7 ± 0.3 b	0.01 ± 0.01 b	91.6 ± 41.3 b	131.5 ± 6.3 a	5.1 ± 0.28 b	463.0 ± 2.6 a	0.74 ± 0.013 a

Letters represent significant differences at $p<0.05$. Capital letters indicate differences between horizons, uncapitalized letters represent significant differences between horizons within each site. Values represent the mean ± 1 SE.

† Thermodynamic Efficiency

List of Figures

Fig. 1. Mineralized CO_2 g^{-1} OC during a 100-day mineralization experiment (a) and mineralized CO_2 normalized to microbial abundance after 100-days of incubation (b) between Ah and Ahb horizons. Bars represent the mean (n=5), error bars represent ± 1 SE, and letters indicate significant differences between horizons at $p < 0.05$.

Fig. 2. Non-metric multidimensional scaling analysis of the microbial community (mol%) from samples after 100-days of incubation in Ah and Ahb horizons at each site. Labeled vectors are significantly correlated ($p<0.001$; $r>0.5$) between variables and ordination sources while length of arrow indicates strength of correlation with longer arrows having stronger correlations. GP- Gram positive bacteria; AMF- arbuscular mycorrhizal fungi. Bars represent the mean (n=20) of total phospholipid fatty acid (PLFA) abundance in the Ah and Ahb horizons. Error bars represent ± 1 SE, and letters represent significant differences between horizons at $p < 0.05$.

Fig. 3. Potentially mineralizable C between sites in the Ah (a) and Ahb (b) horizons. Site order represents highest sand content on left and least sand content on right. Bars represent means (n = 4), error bars represent ± 1 SE, and letters represent significant differences at $p < 0.05$ between sites.

Fig. 4. Heat flow from glucose-amended soils of Ah and Ahb horizons from Swift Current (a), St. Denis (b), Bruno (c), Cudworth (d), and Gronlid (e) over a 48-hour isothermal calorimetry experiment.

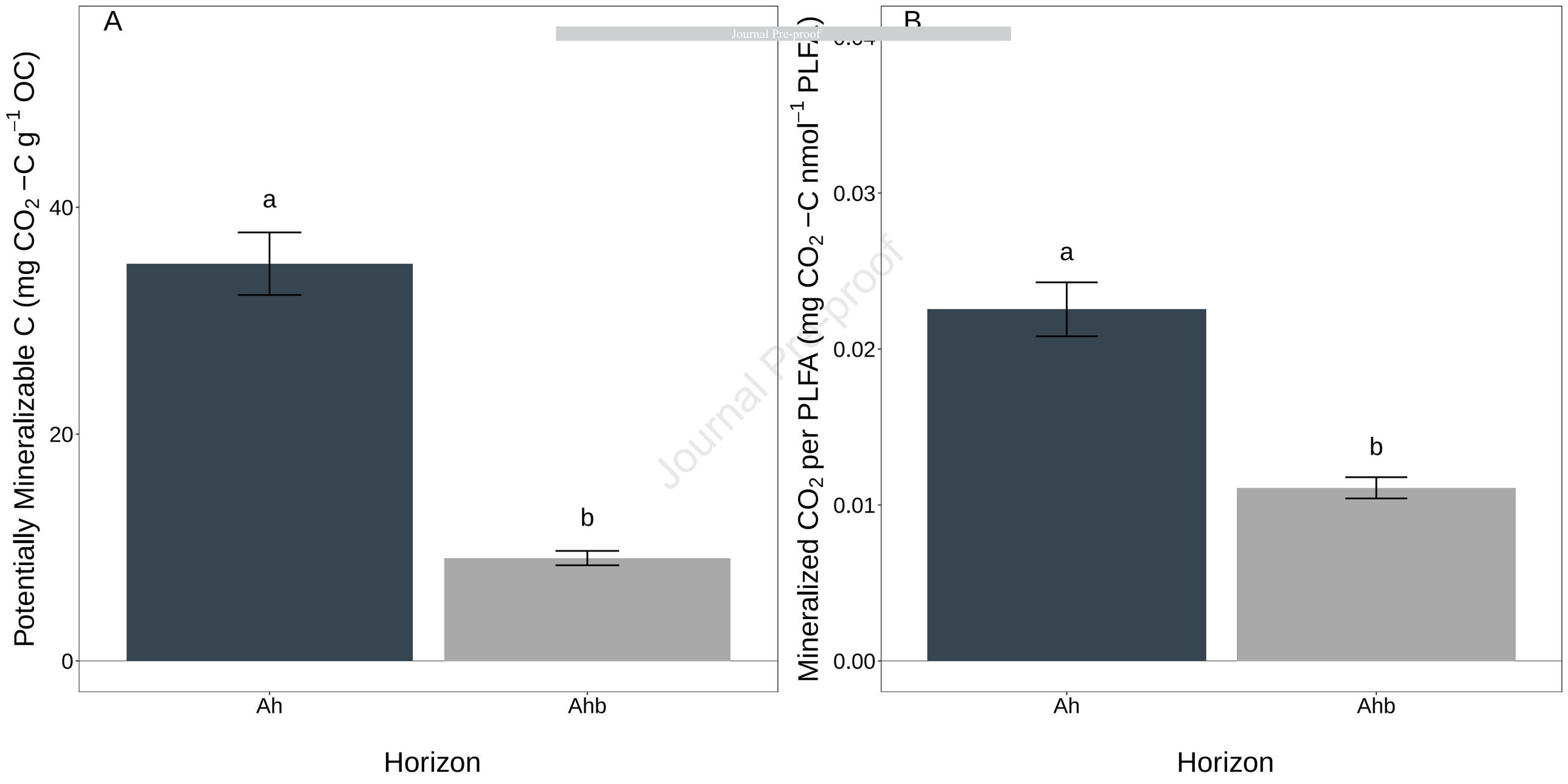

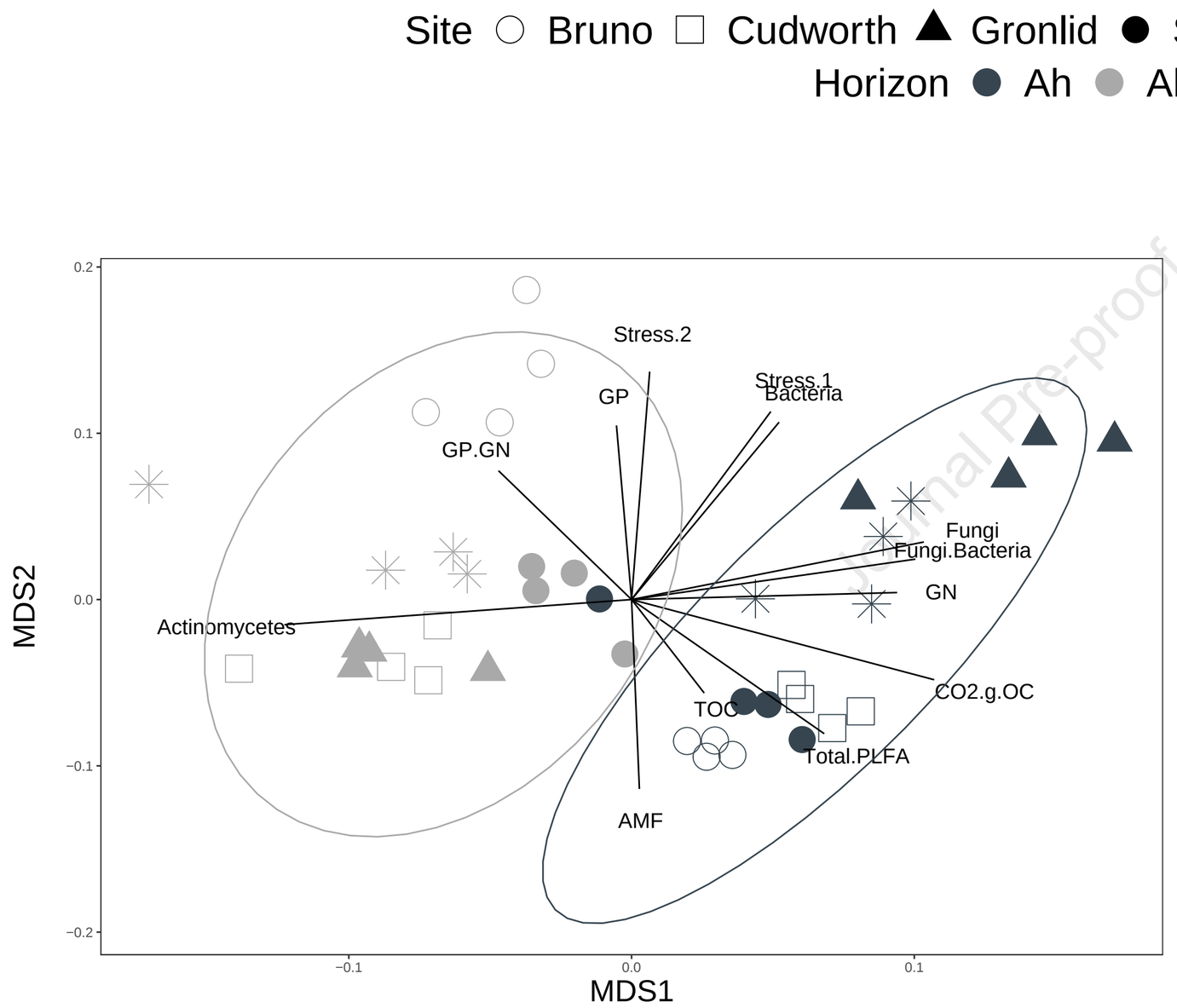

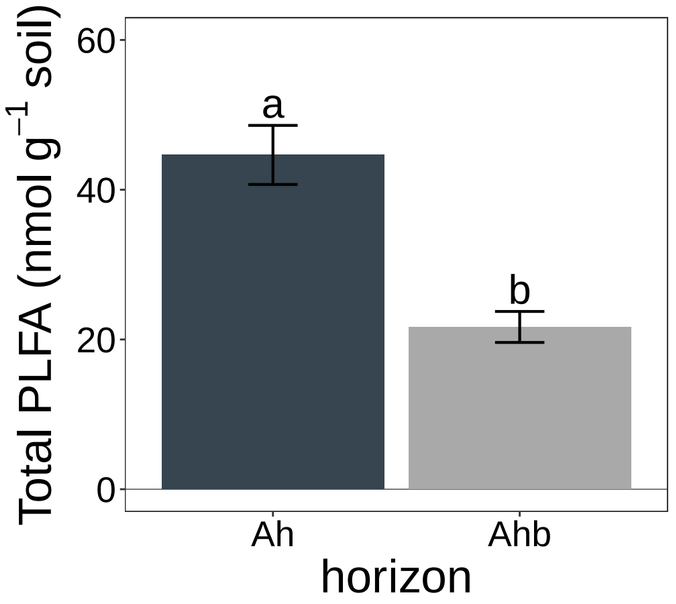

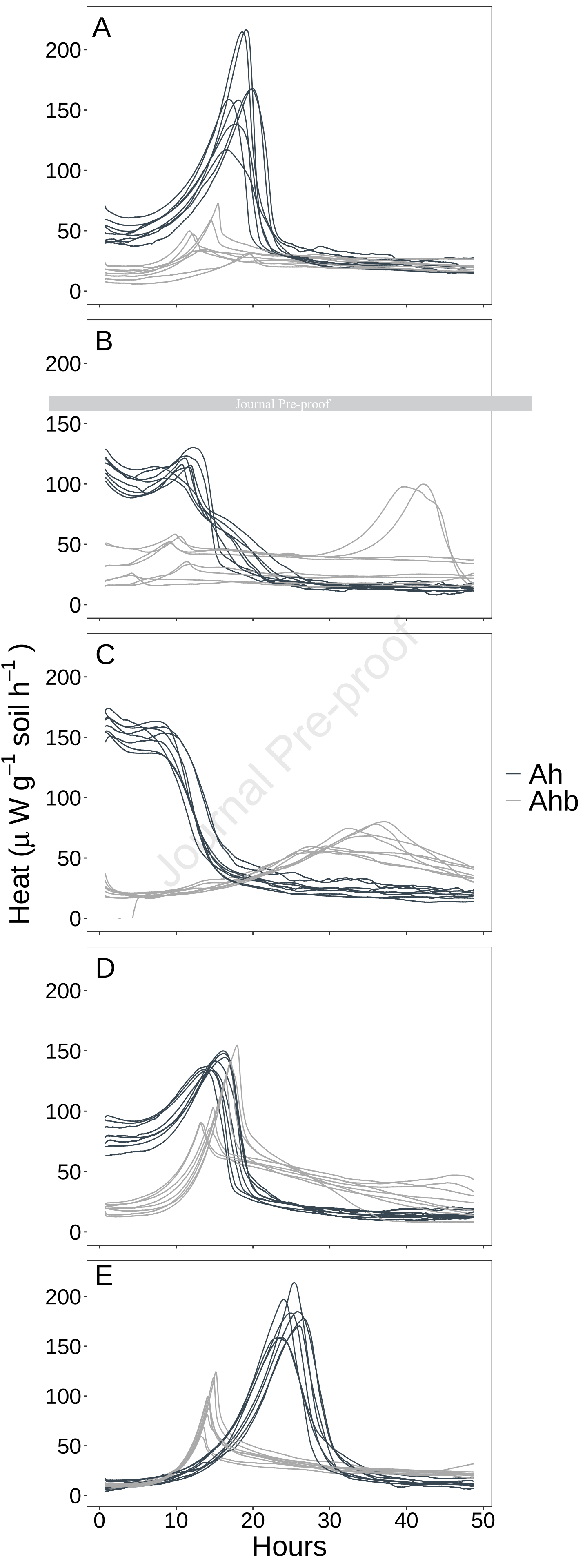

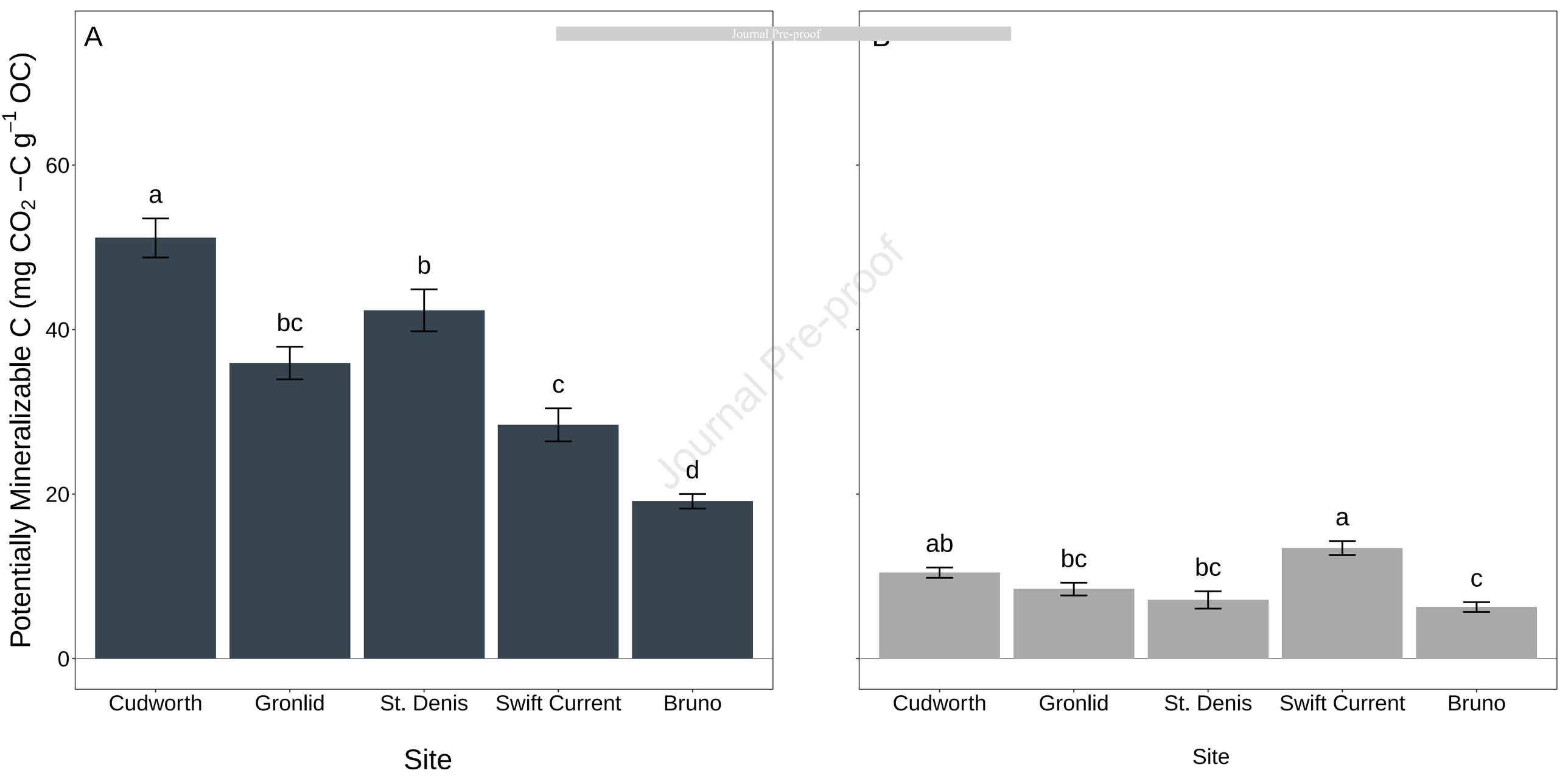

Highlights:

- Higher C persistence in buried vs. surface horizons
- Unique microbial community at depth shifted minimally when incubated
- Less heat dissipation and CO_2 from buried vs. surface horizons
- Similar necromass and high basal calorespirometric ratios in Ahb suggest C recycling
- Microbial adaptation and repeated C turnover led to increased C persistence

Declaration of interests

☒ The authors declare that they have no known competing financial interests or personal relationships that could have appeared to influence the work reported in this paper.

☐ The authors declare the following financial interests/personal relationships which may be considered as potential competing interests: